CHEMISTRY
AN ASIAN JOURNAL
www.chemasianj.org

Accepted Article

Title: Cyclometalated Iridium(III) Bipyridine-Phenylboronic Acid Complexes as Luminescent Probes for Sialic Acids and Bioimaging Reagents

Authors: Hua-Wei Liu, Wendell Ho-Tin Law, Lawrence Cho-Cheung Lee, Jonathan Chun-Wai Lau, and Kenneth Kam-Wing Lo

To be cited as: *Chem. Asian J.* 10.1002/asia.201700359

Link to VoR: http://dx.doi.org/10.1002/asia.201700359

A Journal of

ACES
Asian Chemical Editorial Society

A sister journal of **Angewandte Chemie** and **Chemistry – A European Journal**

WILEY-VCH

10.1002/asia.201700359

WILEY-VCH

Cyclometalated Iridium(III) Bipyridine–Phenylboronic Acid Complexes as Luminescent Probes for Sialic Acids and Bioimaging Reagents

Hua-Wei Liu, Wendell Ho-Tin Law, Lawrence Cho-Cheung Lee, Jonathan Chun-Wai Lau, and Kenneth Kam-Wing Lo*[a]

Abstract: Sialic acids play important roles in mammalian development, cell-cell attachment, and signaling. Since cancer cells utilize their overexpressed sialylated antigens to propagate metastases, the development of probes for sialic acids is of high importance. Herein, we report three luminescent cyclometalated iridium(III) bipyridine complexes bearing a phenylboronic acid (PBA) moiety. Spectrophotometric titrations revealed that the PBA complexes displayed higher binding affinity to the most common sialic acid *N*-acetylneuraminic acid (Neu5Ac) compared with simple sugars that are commonly found on glycoproteins. Notably, cellular imaging and uptake experiments showed that the PBA complexes were able to recognize cellular sialic acid residues, resulting in more efficient uptake than the boronic acid-free analogues. Additionally, one of the PBA complexes was shown to discriminate between cancerous and noncancerous cells.

Introduction

Sialic acid is a generic term for over 50 structural analogues of neuraminic acid, with the most common member being *N*-acetylneuraminic acid (Neu5Ac, Scheme 1).[1] All sialic acids share a cyclic nine-carbon structure with a carboxyl group at C1, providing them a negative charge under physiological pH. Instead of being an energy source, sialic acids are required for mammalian development, cell-cell attachment, and signaling.[2] Cancer cells use their overexpressed sialylated antigens such as sialyl Lewis X (sLe^x) and sialyl Lewis A (sLe^a) to facilitate interactions with the selectins on platelets, innate immune cells, and endothelium, serving to propagate metastases.[1,3] These findings have attracted much interest in the development of probes for sialic acids. However, the lack of distinct reactive groups in sialic acids is a challenge to the development of molecular probes. Although sialic acids can be recognized by antibodies[1,4] and natural lectins,[1,3b,5] and periodate oxidation with aniline-catalyzed ligation (PAL),[6] these methods have limitations; for example, it is difficult to translate antibodies and lectins to *in vivo* applications due to their immunogenicity and large molecular size, which refrain them from approaching vascular compartments. Also, the PAL method necessitates a non-physiological reaction condition (pH ≤ 5). These requirements restrict the applicability of these methods in recognizing and visualizing sialic acid residues on cell surfaces. Recently, there is a growing interest in the use of phenylboronic acid (PBA) as a recognition unit for cell-surface sialic acids.[6–10] The PBA unit forms a five- or six-membered cyclic ester with the exocyclic polyol function of sialic acid. The PBA–sialic acid esters formed are usually more stable than other PBA–sugar esters at physiological pH (pH 7.4) and even intratumoral pH (pH 6.5).[6–10] Thus, PBA has been incorporated into nanoparticles, gold/metal oxide-coated electrodes, organic compounds, and lanthanide chelates to afford sensors for sialic acids.[7–10] Notwithstanding these developments, the possibility of using luminescent transition metal complexes as probes for sialic acids has not been explored. In view of the interesting photophysical behavior of cyclometalated iridium(III) polypyridine complexes,[11] we anticipate that functionalization of these complexes with a PBA moiety will lead to a new class of luminescent probes and imaging reagents for sialic acids.

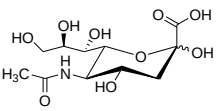

Scheme 1. Structure of Neu5Ac.

Herein, we report three luminescent cyclometalated iridium(III) bipyridyl–PBA complexes $[Ir(N^C)_2(bpy\text{-}TEG\text{-}PBA)](PF_6)\cdot n$HCl (bpy-TEG-PBA = 4-(*N*-(13-(3-boronobenzylamino)-4,7,10-trioxa-tridecanyl)aminocarbonyl-oxy-methyl)-4'-methyl-2,2'-bipyridine; HN^C = 2-phenylpyridine (Hppy), *n* = 0, (**1a**), 2-phenylquinoline, *n* = 0, (Hpq) (**2a**), 2-phenyl-4-quinolinecarboxylic acid (Hpqa), *n* = 1, (**3a**)) (Scheme 2). Their boronic acid-free counterparts $[Ir(N^C)_2(bpy\text{-}TEG\text{-}Bn)](PF_6)\cdot n$HCl (bpy-TEG-Bn = 4-(*N*-(13-benzylamino-(4,7,10-trioxa-tridecanyl)aminocarbonyl)-oxy-methyl)-4'-methyl-2,2'-bipyridine; HN^C = Hppy, *n* = 0, (**1b**), Hpq, *n* = 0, (**2b**), Hpqa, *n* = 1, (**3b**)) were also prepared for comparison studies. The electrochemical and photophysical properties of the complexes were studied. Also, the sialic acid-binding properties of the PBA complexes were investigated by spectrophotometric titrations. Additionally, the lipophilicity, cellular uptake, cytotoxic activity, and bioimaging capability of the complexes were investigated.

[a] Dr. H.-W. Liu, Dr. W. H.-T. Law, L. C.-C. Lee, J. C.-W. Lau, Prof. K. K.-W. Lo
Department of Biology and Chemistry
City University of Hong Kong
Tat Chee Avenue, Kowloon, Hong Kong, P. R. China
E-mail: bhkenlo@cityu.edu.hk
Prof. K. K.-W. Lo
State Key Laboratory of Millimeter Waves, City University of Hong Kong, Tat Chee Avenue, Kowloon, Hong Kong, P. R. China

Supporting information for this article is available on the WWW under http://dx.doi.org/10.1002/asia.201xxxxxx.

Results and Discussion

Synthesis of the ligands and complexes

We selected bpy-TEG-PBA as the diimine ligand (Scheme 2) since the triethylene glycol (TEG) spacer-arm can increase the water solubility, polarity, and biocompatibility of the complexes. Also, the amino group that connects the linker and PBA unit is positively charged at physiological pH, which can facilitate sialic acid recognition through electrostatic interaction.[10a,b,e] The synthesis of bpy-TEG-PBA involved the reaction of carbonate ester bpy-phen-NO_2 with NH_2-TEG-NHBoc, followed by removal of the Boc group to an amine derivative, and its subsequent reaction with formyl PBA pinacol ester (Scheme S1). Complexes **1a** – **3a** were prepared from the reaction of bpy-TEG-PBA with the precursor complex $[Ir_2(N^C)_4Cl_2]$ (Scheme 1). The use of different cyclometalating ligands allows the complexes to exhibit different emission properties, lipophilicity, and cellular uptake behavior. Boronic acid-free complexes **1b** – **3b** were also prepared for comparison studies. The synthesis of the pqa complexes **3a**, **b** required an acidification step, resulting in the secondary amine group of both complexes being isolated as the protonated form (see below). All the complexes were characterized by ESI-MS, ^{1}H NMR spectroscopy, and IR spectroscopy and gave satisfactory elemental analyses.

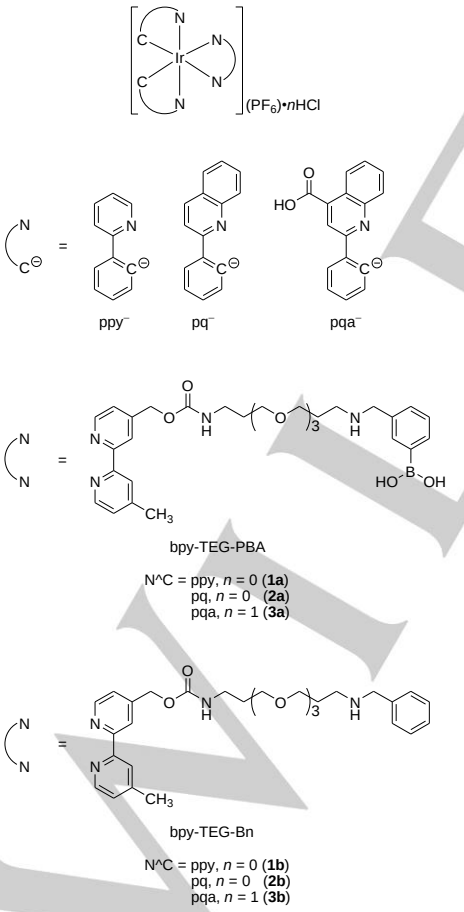

Scheme 2. Structures of the iridium(III) complexes.

Electrochemical properties

The electrochemical properties of the complexes were investigated by cyclic voltammetry and the electrochemical data are summarized in Table 1. The ppy (**1a**, **b**) and pq (**2a**, **b**) complexes exhibited a quasi-reversible oxidation couple at +1.23 to +1.26 V versus SCE, which is assigned to an iridium(IV)/(III) oxidation couple.[12] These complexes displayed an additional quasi-reversible couple or an irreversible wave at +0.95 to +1.00 V, which is associated with the oxidation of the secondary amine moiety.[12a,b,13] Similar to the ppy and pq analogues, the pqa complexes **3a**, **b** showed a metal-centered quasi-reversible couple at +1.35 V (Table 1). The potentials were slightly more positive than those of the ppy and pq complexes as a result of the stronger electron-withdrawing effect of the pqa ligand. The absence of an amine-based quasi-reversible couple/irreversible wave is due to the protonation of the amine group during isolation of the complexes. The first quasi-reversible couple/irreversible wave of all the complexes at −1.44 to −1.49 V are assigned to the reduction of diimine ligands.[12] The reduction couples or waves that occurred at more negative potentials should be associated with the reduction of the cyclometalating ligands.[12,14]

Table 1. Electrochemical data of the iridium(III) complexes at 298 K.[a]

Complex	Oxidation $E_{1/2}$ or E_a/V	Reduction $E_{1/2}$ or E_c/V
1a	+0.97,[b] +1.23[b]	−1.46,[b] −2.04,[c] −2.21[b]
1b	+0.99,[c] +1.25[b]	−1.49,[b] −2.06,[c] −2.22[b]
2a	+0.95,[c] +1.26[b]	−1.45,[b] −1.76,[b] −2.03,[b] −2.33[c]
2b	+1.00,[c] +1.26[b]	−1.49,[b] −1.76,[b] −2.02,[c] −2.37
3a	+1.34[b]	−1.44,[c] −1.54,[b] −1.81,[b] −2.02[b]
3b	+1.35[b]	−1.48,[c] −1.54,[b] −1.83,[b] −2.02[b]

[a] In CH_3CN (0.1 M TBAP), glassy carbon electrode, sweep rate = 100 mV s^{-1}, all potentials are versus SCE. [b] Quasi-reversible couples. [c] Irreversible waves.

Photophysical properties

The electronic absorption spectral data of the iridium(III) complexes in MeOH and buffer solutions at 298 K are listed in Table 2. The electronic absorption spectra of complexes **1a** – **3a** in MeOH at 298 K are shown in Figure 1. All the complexes showed intense spin-allowed ^{1}IL ($\pi \rightarrow \pi^*$) (N^C and N^N) absorption features in the UV region (≈ 255 – 356 nm, ε on the order of 10^4 dm^3 mol^{-1} cm^{-1}) and weaker spin-allowed ^{1}MLCT ($d\pi(Ir) \rightarrow \pi^*$(N^N and N^C))/^{1}LLCT (π(N^C) $\rightarrow \pi^*$(N^N)) absorption shoulders or bands in the visible region (> 344 nm).[12a,c,14c,15] The weaker absorption tailing beyond ≈ 421 nm is assigned to spin-forbidden ^{3}MLCT ($d\pi(Ir) \rightarrow \pi^*$(N^N and N^C))/^{3}LLCT (π(N^C) $\rightarrow \pi^*$(N^N)) transitions.[12a,c,14c,15]

Photoexcitation of the complexes resulted in intense and long-lived green to orange-red emission in fluid solutions under

ambient conditions and in 77-K alcohol glass. The photophysical data are listed in Table 3 and the emission spectra of complexes **1a** – **3a** in MeOH at 298 K are shown in Figure 2. The ppy (**1a**, **b**) and pqa (**3a**, **b**) complexes displayed a broad and featureless emission band with positive solvatochromism in fluid solutions. Upon cooling the samples to 77 K, large blue-shifts of emission maxima were observed, suggestive of a ^{3}MLCT ($d\pi$(Ir) → π^*(N^N/N^C)) emissive state.[12a,c,14c,15,16] In contrast, the pq complexes **2a**, **b** exhibited vibronically structured features and very long emission lifetimes in fluid solutions (Table 3). Also, the emission properties of these two complexes were not very sensitive to the polarity of the solvents, indicative of a ^{3}IL ($\pi \rightarrow \pi^*$) (pq) emissive state.[12a,c,14c,15,16]

Table 2. Electronic absorption spectral data of the iridium(III) complexes at 298 K.

Complex	Solvent	λ_{abs}/nm (ε/dm^3 mol^{-1} cm^{-1})
1a	MeOH	255 (52,160), 275 sh (43,465), 314 sh (18,940), 344 sh (9,445), 385 sh (5,800), 421 sh (3,045)
	Buffer[a]	255 (53,610), 269 sh (48,730), 312 sh (20,285), 344 sh (9,465), 381 sh (6,200), 421 sh (3,770)
1b	MeOH	255 (47,975), 275 sh (40,690), 312 sh (19,465), 344 sh (8,750), 385 sh (5,640), 421 sh (2,950)
	Buffer[a]	255 (46,195), 269 sh (42,075), 312 sh (17,785), 344 sh (8,155), 381 sh (5,415), 421 sh (3,180)
2a	MeOH	262 sh (54,205), 284 sh (51,765), 311 sh (23,910), 336 (25,395), 356 sh (18,705), 438 (5,680)
	Buffer[a]	263 sh (58,340), 284 sh (53,295), 311 sh (26,535), 336 (26,980), 356 sh (23,120), 438 (6,385)
2b	MeOH	262 sh (56,630), 284 sh (54,220), 311 sh (25,230), 336 (26,245), 356 sh (19,150), 438 (5,885)
	Buffer[a]	263 sh (54,130), 284 sh (49,450), 311 sh (24,545), 336 (24,725), 354 sh (19,745), 435 (5,875)
3a	MeOH	264 (48,330), 284 (48,515), 310 sh (22,600), 342 (23,560), 438 (5,280)
	Buffer[b]	267 (46,165), 282 (45,215), 310 sh (24,530), 341 (23,205), 444 (5,790)
3b	MeOH	263 (54,705), 284 (55,395), 308 sh (26,170), 342 (26,455), 440 (5,870)
	Buffer[b]	267 (55,630), 282 (54,570), 310 sh (26,935), 341 (26,585), 444 (5,845)

[a] 50 mM potassium phosphate buffer at pH 7.4/MeOH (7:3, v/v). [b] 50 mM potassium phosphate buffer at pH 7.4/MeOH (9:1, v/v).

Table 3. Photophysical data of the iridium(III) complexes.

Complex	Medium (*T*/K)	λ_{em}/nm	τ_o/μs	Φ_{em}
1a	MeOH (298)	583	0.32	0.048
	H_2O[a] (298)	590	0.10	0.015
	Buffer[b] (298)	589	0.11	0.015
	Glass[c] (77)	473, 500 (max), 547 sh	4.74	
1b	MeOH (298)	585	0.37	0.069
	H_2O[a] (298)	593	0.13	0.021
	Buffer[b] (298)	591	0.13	0.021
	Glass[c] (77)	473, 505 (max), 544 sh	5.13	
2a	MeOH (298)	554, 601 sh	2.66	0.27
	H_2O[a] (298)	557, 602 sh	2.04	0.25
	Buffer[b] (298)	554, 601 sh	1.88	0.22
	Glass[c] (77)	538 (max), 580, 632 sh	7.12	
2b	MeOH (298)	555, 601 sh	2.78	0.28
	H_2O[a] (298)	555, 603 sh	2.02	0.24
	Buffer[b] (298)	557, 601 sh	1.84	0.21
	Glass[c] (77)	541 (max), 581, 630 sh	8.22	
3a	MeOH (298)	587	1.63	0.28
	H_2O[d] (298)	599	0.34	0.012
	Buffer[e] (298)	598	0.36	0.039
	Glass[c] (77)	561, 611 sh	4.44	
3b	MeOH (298)	586	1.50	0.23
	H_2O[d] (298)	599	0.36	0.010
	Buffer[e] (298)	598	0.37	0.057
	Glass[c] (77)	563, 613 sh	4.45	

[a] H_2O/MeOH (7:3, v/v). [b] 50 mM potassium phosphate buffer at pH 7.4/MeOH (7:3, v/v). [c] EtOH/MeOH (4:1, v/v). [d] H_2O/MeOH (9:1, v/v). [e] 50 mM potassium phosphate buffer at pH 7.4/MeOH (9:1, v/v).

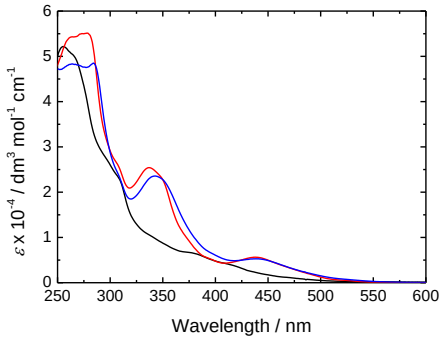

Figure 1. Electronic absorption spectra of complexes **1a** (black), **2a** (red), and **3a** (blue) in MeOH at 298 K.

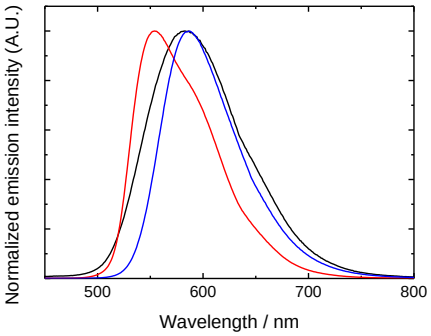

Figure 2. Emission spectra of complexes **1a** (black), **2a** (red), and **3a** (blue) in MeOH at 298 K.

Sugar-binding studies

The sugar-binding properties of the complexes were studied by spectrophotometric titrations. Upon addition of Neu5Ac, the absorbance of the PBA complexes **1a** – **3a** at 309 – 342 nm was decreased by ≈ 3 to 10% after correction for dilution effect. Similar changes were not observed for the boronic acid-free complexes **1b** – **3b**. The absorption titration curves for complexes **3a**, **b** with Neu5Ac are illustrated in Figure 3. Since the boronic acid-free analogues did not display a comparable decrease, we attribute the absorbance changes to the binding of Neu5Ac to the PBA unit of complexes **1a** – **3a**. The formation of adducts was supported by ESI-MS (Figure S1). The binding affinity of the PBA complexes to D-glucose, D-galactose, and D-mannose, which are commonly found in eukaryotic glycoproteins,[17] was also investigated. Upon addition of D-glucose, D-galactose, and D-mannose, complexes **1a** – **3a** required a much higher concentration of sugars to reach the end point (Figures S2 – S4), indicating that the PBA complexes are more selective to Neu5Ac among the sugars. Treatment of the titration data of the PBA complexes with the sugars using a 1:1 binding model gave satisfactory fits.[18] The plots of $A_o/(A_o - A)$ vs. $[Sugar]^{-1}$ (Sugar = Neu5Ac, D-glucose, D-galactose, and D-mannose) for complex **3a** and the corresponding theoretical fits are shown in Figure S5 as an example. The log K_b values for the binding of sugars to the PBA complexes **1a** – **3a** are listed in Table 4. The log K_b values for the binding of Neu5Ac range from 3.61 to 3.85 and are larger than those of D-glucose (from 1.68 to 2.92), D-galactose (from 2.63 to 3.17), and D-mannose (from 2.16 to 3.34). These values follow the order: Neu5Ac > D-galactose ≈ D-mannose > D-glucose, which is in accordance with those reported in related studies.[9a,c,10a,c,d] Variation of the cyclometalating ligands did not substantially change the binding affinity of the complexes to Neu5Ac and the other three sugars. Additionally, the log K_b values for the binding of Neu5Ac to the PBA complexes are much larger than that of unmodified PBA (log K_b ≈ 1.30).[19] It is well established that the optimal PBA-sugar binding requires basic conditions where the concentration of the boronate anion is maximal.[19,20] Also, recent studies have shown that the presence of an aminomethyl group at the *meta* position of PBA enhances the specificity and stability of the PBA-Neu5Ac adduct through a cooperative binding mode (Scheme 3).[10a,b,e] Thus, the higher binding affinity of the PBA complexes to Neu5Ac than other sugars studied (and the stronger Neu5Ac-binding of the PBA complexes compared with unmodified PBA) should be due to cooperative two-site binding through (1) PBA ester formation with the vicinal diol of Neu5Ac and (2) electrostatic interaction between the ammonium group of the complexes and carboxylate of Neu5Ac.

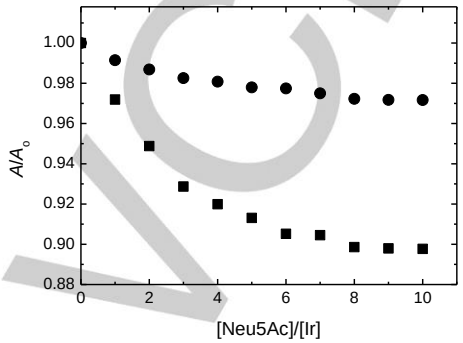

Figure 3. Results of spectrophotometric titrations of complexes **3a** (squares) and **3b** (circles) (50 μM), respectively, with Neu5Ac in 50 mM potassium phosphate buffer at pH 7.4/DMSO (9:1, v/v) at 298 K. Absorbance was monitored at 342 nm and corrected for dilution effect.

Table 4. Log K_b values for the binding of sugars to complexes **1a** – **3a** in 50 mM potassium phosphate buffer at pH 7.4/DMSO (9:1, v/v) at 298 K.

Complex	Neu5Ac	D-Glucose	D-Galactose	D-Mannose
1a	3.61	2.85	3.17	3.21
2a	3.85	2.92	3.05	3.34
3a	3.62	1.68	2.63	2.16

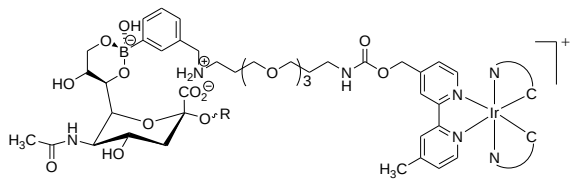

Scheme 3. Schematic representation of sialic acid recognition by the iridium(III) PBA complexes via a cooperative binding mode.

Effects of pH values on emission behavior

The possible effects of pH on the emission of the complexes were studied by emission spectroscopy. When the pH values of the solutions were tuned from high to low, the emission of the ppy (**1a**, **b**) and pq (**2a**, **b**) complexes did not display any pH-dependence even at pH values lower than the pK_a of benzylamine and that of PBA (≈ 9.40 and 8.70, respectively) (Figures S6 and S7).[21] These findings are reasonable in view of the lack of electronic communication between the PBA/benzylamine moiety and the iridium(III) polypyridine core.

In contrast, the effects of pH on the emission properties of the pqa complexes **3a**, **b** were more pronounced. At pH between 12 and 7, the complexes exhibited intense orange-red emission (λ_{em} = 589 nm) with insignificant pH-dependence. Upon decreasing the pH to < 7, the emission bands of the complexes were bathochromically shifted and displayed reduced intensities (Figure 4). The emission intensities at pH > 7 were ≈ 10- to 25-fold higher than those at pH < 3 (Figure 5). Nonlinear least-square fits of the titration curves of complexes **3a**, **b** in the low-pH region yielded apparent pK_a values of 4.57 ± 0.01 and 4.37 ± 0.02, respectively. The emission quenching is attributed to the protonation of the carboxylate of pqa ligands of the complexes. The pK_a values are slightly smaller than that of [Ir(TPAQCOOH)$_2$(pic)] (pK_a = 5.16 ± 0.05) (HTPAQCOOH = 2-((4-diphenylamino)phenyl)-4-quinolinecaboxylic acid; pic = picolinate),[22] which is probably due to the absence of the electron-donating diphenylamine moiety in complexes **3a**, **b**. Since it is well known that the ^{3}MLCT (dπ(Ir) → π^*(N^C)) emission intensity is much lower than that of ^{3}IL emission in related iridium(III) complexes,[23] the observed emission quenching upon decreasing the pH should originate from the increased ^{3}MLCT (dπ(Ir) → π^*(pqa)) character in the emissive states of complexes **3a**, **b**. This is also supported by the fact that protonation of the carboxylate group will favor charge-transfer from the iridium(III) center to the cyclometalating ligands. On the basis of the titration results, the pqa ligands of complexes **3a**, **b** exist in the deprotonated form in the biologically relevant pH range (pH ≈ 7.20 – 8.10).

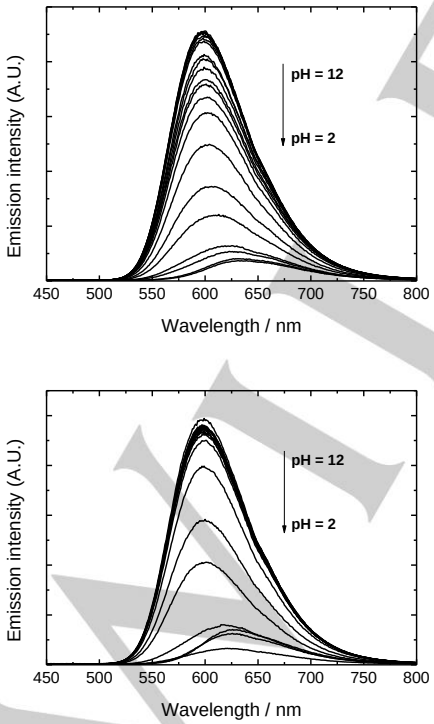

Figure 4. Emission spectral traces of complexes **3a** (top) and **3b** (bottom) (50 μM) in aerated 100 mM KCl(aq)/MeOH (9:1, v/v) at 298 K upon decreasing the pH of the solutions.

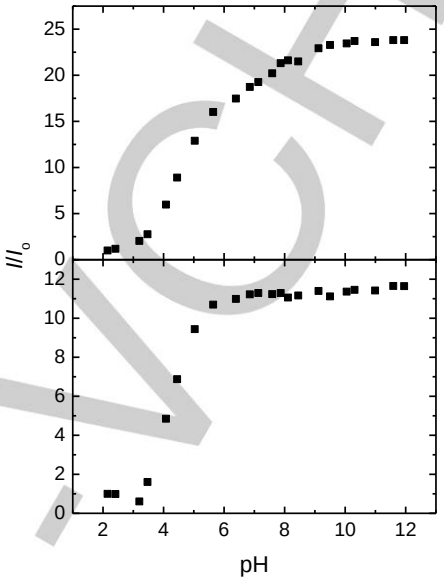

Figure 5. Results of the pH titrations of complexes **3a** (top) and **3b** (bottom) (50 μM) in aerated 100 mM KCl(aq)/MeOH (9:1, v/v) at 298 K. The emission intensity of the complexes at pH = 2 was set as the reference point (I_o).

Lipophilicity and cellular uptake efficiency

The lipophilicity of the complexes was determined by the shake-flask method, and the results expressed as log $P_{o/w}$ values are listed in Table 5. The log $P_{o/w}$ values ranged from 0.71 to 2.18 and were strongly dependent on the cyclometalating ligands and their substituents. The log $P_{o/w}$ values of the ppy complexes **1a**, **b** (1.17 and 1.32, respectively) were lower than those of their pq counterparts **2a**, **b** (1.96 and 2.18, respectively) owing to the hydrophobic nature of the pq ligands. Also, the pqa complexes **3a**, **b** (log $P_{o/w}$ = 0.71 and 0.82, respectively) were much less lipophilic than the pq analogues, reflecting the effect of the polar carboxyl groups. The polar boronic acid group rendered complexes **1a** – **3a** less lipophilic than their boronic acid-free counterparts complexes **1b** – **3b**, respectively.

Table 5. Lipophilicity and cellular uptake of the iridium(III) complexes.

Complex	Lipophilicity (log $P_{o/w}$)[a]	Amount of iridium/fmol[b]
1a	1.17	2.04 ± 0.11
1b	1.32	1.79 ± 0.21
2a	1.96	7.17 ± 0.26
2b	2.18	6.63 ± 0.31
3a	0.71	0.86 ± 0.06
3b	0.82	0.58 ± 0.02

[a] Log $P_{o/w}$ is defined as the logarithmic ratio of the concentration of the complex in octan-1-ol to that in an aqueous NaCl solution (0.9%, w/v). [b] Amount of iridium associated with an average HepG2 cell upon incubation with the complexes (25 μM) at 37°C for 1 h.

The uptake of all the complexes by HepG2 cells was determined by ICP-MS measurements. Upon incubation with the complexes (25 μM) at 37°C for 1 h, an average HepG2 cell was found to contain 0.58 to 7.17 fmol of iridium (Table 5), which is comparable to those reported in the cellular uptake studies of other inorganic complexes.[24] The uptake efficiency of the complexes followed the orders: **3a** < **1a** < **2a** and **3b** < **1b** < **2b**, which is in accordance with their lipophilicity (Table 5). Importantly, the PBA complexes revealed higher cellular uptake compared with the boronic acid-free complexes. Similar enhanced uptake has been observed when cells that express *N*-azidoacetyl sialic acid are incubated with dibenzocyclooctyne derivatives.[25] Since hepatic cancer cells such as HepG2 cells express upregulated levels of sialylated antigens,[9b,e,26] it is likely that the higher cellular uptake of the PBA complexes is assisted by their interactions with cellular sialic acid moieties.

Cytotoxic activity

The cytotoxic activity of all the complexes was investigated by the MTT assay,[27] where the dose dependence of surviving HepG2 cells after exposure to the complexes for 1 h was evaluated. The results showed that within a concentration range of 6.25 – 12.5 μM, all the complexes were noncytotoxic (percentage of surviving cells ≥ 95%) irrespective of their lipophilicity and cellular uptake efficiencies (Figure S8). Upon increasing the concentrations to 25 – 50 μM, only the cells treated with the pq complexes **2a**, **b** exhibited a noticeable decrease in viability, which is in line with their highest cellular uptake efficiencies among the complexes (Table 5). This effect was more obvious when the concentration was further increased to 100 μM, where the percentage of surviving cells treated with the pq complexes reduced to ≈ 30%, which is 2- to 5-fold lower than that of the ppy and pqa complexes, respectively. The photocytotoxic activity of the complexes was also examined (Figure S9). The results showed that the viability of the cells treated with complexes **1a**, **b** and **3a**, **b** (25 μM, 1 h) remained high (> 70%) under both dark and light conditions (λ_{irr} = 365 nm, 10 min), probably due to the low cellular uptake efficiency of the complexes (Table 5). In contrast, complex **2a** displayed noticeable photocytotoxic effect (cell viability decreased from 65.6 to 7.3% upon irradiation), while the most lipophilic complex **2b** caused extensive cell death with or without irradiation.

Cellular sialic acid-recognition studies

Since the PBA complexes **1a** – **3a** showed interesting Neu5Ac-binding ability, their capability of recognizing sialic acid residues expressed on HepG2 cell membrane was evaluated by laser-scanning confocal microscopy. Treatment of the cells with complexes **1a** and **2a** (25 μM) at 37°C under a 5% CO_2 atmosphere for 1 h led to strong intracellular emission. Similar results were observed in the cells incubated with the boronic acid-free complexes **1b** and **2b**, indicative of very efficient cellular internalization (Figure S10). Additionally, the more lipophilic complex **2a** was internalized into the cells much faster than complex **1a**, as revealed by the time-dependent imaging studies (Figure S11). Similar to many other cyclometalated iridium(III) polypyridine complexes, these complexes were not localized in the nucleus. The ppy complexes were diffusely distributed in the cytoplasm with punctate staining whereas the pq complexes fully stained the cytoplasm. Although complexes **1a** and **2a** did not appear to bind to cell-surface sialic residues, it is noteworthy that co-incubation of the cells with these complexes and free Neu5Ac resulted in reduced intracellular emission intensity (Figure 6), whereas similar inhibition was not observed for their boronic acid-free counterparts complexes **1b** and **2b** (Figure S12). These results offer strong evidence that the uptake of complexes **1a** and **2a** was facilitated by their interactions with sialic acid residues on the cell membrane.

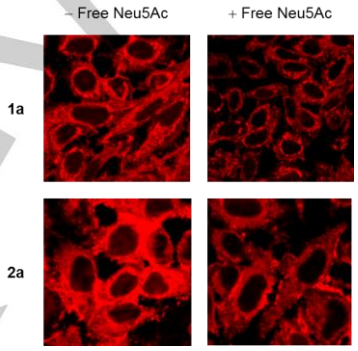

Figure 6. Laser-scanning confocal images of HepG2 cells upon incubation with complexes **1a** and **2a** (25 μM, 1 h) in PBS/DMSO (99:1, v/v) containing 1% FBS in the absence (left) and presence (right) of free Neu5Ac (500 μM, 1 h) at 37°C, respectively.

The cellular uptake of complexes **1a**, **b** and **2a**, **b** was studied in more detail. In an attempt to alter membrane fluidity (and/or decrease cellular energy utilization), HepG2 cells were incubated at 4°C prior to treatment with the complexes.[28] The intracellular emission intensities of the treated cells were negligible (Figures S13 and S14). Upon preincubation with the cytoskeletal inhibitor colchicine or the oxidative phosphorylation inhibitor 3-chlorophenylhydrazone (CCCP), the emission intensities of the cells loaded with the ppy complexes decreased substantially (Figure S13) whereas the pq complexes did not bring a similar change (Figure S14). On the basis of these results, the cellular uptake of the ppy complexes should occur through an energy-dependent pathway, which is possibly endocytosis. Also, the effect of lipophilicity of the pq complexes appeared to play an important role in their cellular uptake, suggesting passive diffusion as a major pathway.[28,29]

On contrary to complexes **1a** and **2a**, incubation of HepG2 cells with complex **3a** under the same conditions led to cell membrane staining with much weaker cytoplasmic emission (Figure 7, top left). Importantly, cells that were loaded with the control complex **3b** gave no emission (Figure 7, bottom left). The absence of extensive cytoplasmic staining should be a result of the limited uptake of complexes **3a**, **b** due to their much

lower lipophilicity and electrostatic repulsion between their carboxylate groups and the phospholipid bilayers. Interestingly, in the presence of free Neu5Ac, the cells treated with complex **3a** no longer displayed cell membrane staining (Figure 7, top middle). A similar observation was obtained when the cells were pretreated with neuraminidase, which specifically catalyzes the hydrolysis of α(2,3) sialic acid linkages, before incubation with complex **3a** (Figure 7, top right). Also, ICP-MS measurements revealed that the cellular uptake of complex **3a** by Neu5Ac- and neuraminidase-treated cells was decreased by ≈ 40 and 30%, respectively (Figure 8, red bars). In contrast, the cells treated with complex **3b** under the same conditions did not exhibit any noticeable difference (Figure 7, bottom and Figure 8, blue bars). On the basis of these findings, we can conclude that the membrane staining by complex **3a** was due to its interaction with the sialic acid residues on the cell membrane. Additionally, upon increasing the incubation time, the cells displayed intense cytoplasmic staining, indicating the internalization of labeled cell-surface glycans and/or the free complex.[25]

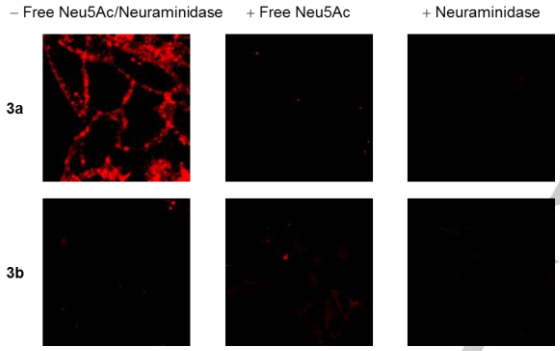

Figure 7. Laser-scanning confocal images of HepG2 cells upon incubation with complexes **3a**, **b** (25 μM, 1 h) at 37°C without any treatment (left), simultaneously treated with free Neu5Ac (500 μM, 1 h) (middle), and pretreated with neuraminidase (0.1 U mL^{-1}, 1 h) (right), respectively.

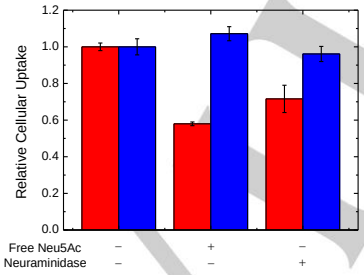

Figure 8. Relative uptake of iridium by HepG2 cells upon incubation with complexes **3a** (red) and **3b** (blue) (25 μM) at 37°C for 1 h with or without treatment with free Neu5Ac (500 μM) and neuraminidase (0.1 U mL^{-1}) for 1 h. The uptake of complexes **3a**, **b** in the absence of Neu5Ac and neuraminidase was set as respective reference points.

Our next question is whether complex **3a** can distinguish cells with different expression levels of membrane-bound sialic acid residues. To address this point, we selected HEK293T cells as a normal cell model, which is known to express a lower level of cancer-associated glycans.[30] We found that HEK293T cells loaded with complex **3a** displayed negligible cellular emission (Figure S15, left), which is very different to the case of HepG2 cells (Figure 7, top left) under the same incubation conditions. Additionally, ICP-MS measurements showed that the cellular uptake of complex **3a** by HEK293T cells was ≈ 5.2-fold lower than that by HepG2 cells (Figure 9, red bars). Again, treatment of HEK293T cells with complex **3b** did not result in any noticeable cellular emission (Figure S15, right and Figure 9, blue bars). These interesting findings illustrate that complex **3a** is capable of recognizing cell-surface sialic acid residues and exhibits cellular discrimination ability.

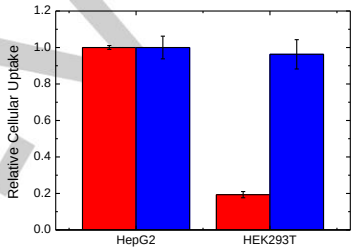

Figure 9. Relative uptake of iridium by HepG2 and HEK293T cells upon incubation with complexes **3a** (red) and **3b** (blue) (25 μM) at 37°C for 1 h. The uptake of complexes **3a**, **b** by HepG2 cells was set as respective reference points.

Conclusions

In this work, three luminescent cyclometalated iridium(III) bipyridine complexes functionalized with a PBA moiety and their boronic acid-free counterparts were synthesized and characterized. Their electrochemical, photophysical, lipophilicity cellular uptake efficiency, and cytotoxic activity were investigated. The binding of the PBA complexes to various sugars was also studied, and the results indicated that the complexes were selective towards Neu5Ac over other sugars. The emission of all the complexes was pH-insensitive in the biologically relevant range (pH ≈ 7.20 – 8.10). Interestingly, ICP-MS analyses revealed that the ppy (**1a**, **b**) and pq (**2a**, **b**) complexes were internalized into live HepG2 cells much more efficiently than their pqa counterparts (**3a**, **b**), which was closely related to the lipophilicity of the complexes. The cytotoxic effects of the complexes toward HepG2 cells were negligible at the concentration used for live-cell imaging (25 μM). Also, laser-scanning confocal images showed that the PBA complexes **1a** and **2a** stained the cell cytoplasm readily whereas complex **3a** was located on the surface of plasma membrane. Importantly, experiments involving free Neu5Ac and neuraminidase confirmed that the membrane staining was due to the interaction of complex **3a** with cell-surface sialic acids. Furthermore, complex **3a** was found to be capable of distinguishing the

cancerous HepG2 and noncancerous HEK293T cells. All these findings demonstrated the innovative applications of the iridium(III) bipyridine–PBA complexes as luminescent probes for tumor-associated sialic acid residues at physiological pH via the borate ester chemistry. The cancer cell-targeting properties of related photofunctional complexes are expected to inspire the development of novel therapeutics.

Experimental Section

General considerations

All solvents were of analytical reagent grade and purified according to standard procedures.[31] All buffer components were of biological grade and used as received. 4,4'-Dimethyl-2,2'-bipyridine, selenium oxide, sodium metabisulfite, 4,7,10-trioxa-1,13-tridecanediamine, di-*tert*-butyl dicarbonate, NH_4OH, pinacol, iridium(III) chloride hydrate, Hppy, Hpq, Hpqa, $LiOH{\cdot}H_2O$, tetra-*n*-butylammonium hexafluorophosphate (TBAP), KOH, and MTT were purchased from Aldrich. Sodium carbonate, $NaBH_4$, 4-nitrophenyl chloroformate, pyridine, Et_3N, trifluoroacetic acid (TFA), NaCl, $MgSO_4$, 3-formylphenylboronic acid, benzaldehyde, KPF_6, amberlite IR120 H resin, ferrocene, D-glucose, D-galactose, D-mannose, KCl, octan-1-ol, colchicine, and CCCP were obtained from Acros. Neu5Ac was purchased from Calbiochem. Neuraminidase from *Clostridium perfringens* was obtained from Sigma. All these chemicals were used without further purification except that TBAP was recrystallized from hot ethanol and dried *in vacuo* at 110°C before use. The iridium dimers $[Ir_2(N\text{^}C)_4Cl_2]$ (HN^C = Hppy, Hpq, 2-phenylcinchoninic acid methyl ester (Hpqe)), 4-formyl-4'-methyl-2,2'-bipyridine (bpy-CHO), 4-hydroxylmethyl-4'-methyl-2,2'-bipyridine (bpy-OH), *N*-(*tert*-butoxycarbonyl)amino-4,7,10-trioxa-1,13-tridecanediamine (NH_2-TEG-NHBoc), and 3-formylphenylboronic acid pinacol ester were prepared as previously reported.[12c,15a,16,32] Autoclaved Milli-Q water was used for preparation of the aqueous solutions. HepG2 and HEK293T cells were obtained from American Type Culture Collection. Dulbecco's modified Eagle's medium (DMEM), glucose-free DMEM, phosphate buffered saline (PBS), fetal bovine serum (FBS), trypsin-EDTA, and penicillin/streptomycin were purchased from Invitrogen. The instruments for characterization, as well as electrochemical and photophysical measurements, have been described previously.[12b] The procedures for emission quantum yield measurements,[33] MTT assays,[27] ICP-MS,[12b] and live-cell confocal imaging[12b,25c,34] were reported previously.

4-(4-Nitrophenyloxycarbonyl-oxy-methyl)-4'-methyl-2,2'-bipyridine (bpy-phen-NO_2)

A mixture of bpy-OH (667 mg, 3.34 mmol), 4-nitrophenyl chloroformate (1.34 g, 6.68 mmol), and pyridine (1.35 mL, 16.7 mmol) in CH_2Cl_2 (20 mL) was stirred at room temperature under an inert atmosphere of nitrogen for 2 h. The solution was washed with H_2O (100 mL × 3) and then saturated NaCl solution (100 mL × 2). The combined organic extract was dried over $MgSO_4$, filtered, and the solvent was removed by rotary evaporation to give a purple solid. The crude product was purified by column chromatography on silica gel using EtOAc as the eluent. The product bpy-phen-NO_2 was subsequently isolated as a white solid. Yield: 1.07 g (88%). ^{1}H NMR (400 MHz, $CDCl_3$, 298 K, TMS): δ = 8.72 (d, J = 5.0 Hz, 1H, H6 of bpy), 8.55 (d, J = 4.8 Hz, 1H, H6' of bpy), 8.45 (s, 1H, H3 of bpy), 8.30 – 8.27 (m, 2H, H3 and H5 of phenyl ring), 8.26 (s, 1H, H3' of bpy), 7.42 – 7.40 (m, 2H, H2 and H6 of phenyl ring), 7.36 (d, J = 4.8 Hz, 1H, H5 of bpy), 7.17 (d, J = 4.8 Hz, 1H, H5' of bpy), 5.39 (s, 2H, CH_2), 2.45 ppm (s, 3H, CH_3). MS (ESI^+): m/z: 366 $[M + H]^+$.

4-(*N*-(13-*N*'-(*tert*-Butoxycarbonyl)amino-4,7,10-trioxa-tridecanyl)aminocarbonyl-oxy-methyl)-4'-methyl-2,2'-bipyridine (bpy-TEG-NHBoc)

A mixture of bpy-phen-NO_2 (438 mg, 1.20 mmol), NH_2-TEG-NHBoc (767 mg, 2.39 mmol), and Et_3N (1 mL) in CH_2Cl_2 (10 mL) was stirred at room temperature under an inert atmosphere of nitrogen for 24 h. The solvent was removed by rotary evaporation to give a yellow oil. The crude product was purified by column chromatography on silica gel using EtOAc as the eluent. The product bpy-TEG-NHBoc was subsequently isolated as a colorless oil. Yield: 613 mg (93%). ^{1}H NMR (400 MHz, $CDCl_3$, 298 K, TMS): δ = 8.63 (d, J = 4.8 Hz, 1H, H6 of bpy), 8.51 (d, J = 5.2 Hz, 1H, H6' of bpy), 8.33 (s, 1H, H3 of bpy), 8.21 (s, 1H, H3' of bpy), 7.26 (d, J = 6.0 Hz, 1H, H5 of bpy), 7.14 (d, J = 4.8 Hz, 1H, H5' of bpy), 5.18 (s, 2H, CH_2 on C4 of bpy), 3.64 – 3.45 (m, 12H, CH_2O), 3.35 – 3.31 (m, 2H, CONHCH_2), 3.18 (d, J = 6.0 Hz, 2H, CH_2NHBoc), 2.43 (s, 3H, CH_3 of bpy), 1.81 – 1.78 (m, 2H, $CONHCH_2CH_2$), 1.70 (t, J = 6.0 Hz, 2H, CH_2CH_2NHBoc), 1.41 ppm (s, 9H, CH_3 of Boc). MS (ESI^+): m/z: 569 $[M + Na]^+$.

4-(*N*-(13-Amino-4,7,10-trioxa-tridecanyl)aminocarbonyl-oxy-methyl)-4'-methyl-2,2'-bipyridine (bpy-TEG-NH_2)

A mixture of bpy-TEG-NHBoc (563 mg, 1.03 mmol) and TFA (2 mL) in CH_2Cl_2 (20 mL) was stirred at room temperature under an inert atmosphere of nitrogen for 2 h. The combined organic layer was neutralized by addition of NH_4OH. The mixture was extracted with CH_2Cl_2 (100 mL × 2). The solution was washed with H_2O (100 mL × 3) and then saturated NaCl solution (100 mL × 2). The combined organic extract was dried over $MgSO_4$, filtered, and the solvent was removed by rotary evaporation. The product bpy-TEG-NH_2 was subsequently isolated as a colorless oil. Yield: 401 mg (87%). ^{1}H NMR (400 MHz, $CDCl_3$, 298 K, TMS): δ = 8.56 (d, J = 4.8 Hz, 1H, H6 of bpy), 8.45 (d, J = 5.2 Hz, 1H, H6' of bpy), 8.28 (s, 1H, H3 of bpy), 8.15 (s, 1H, H3' of bpy), 7.19 (d, J = 3.6 Hz, 1H, H5 of bpy), 7.07 (d, J = 4.8 Hz, 1H, H5' of bpy), 6.10 (s, 1H, CONH), 5.11 (s, 2H, CH_2 on C4 of bpy), 3.57 – 3.41 (m, 12H, CH_2O), 3.28 – 3.23 (m, 2H, CONHCH_2), 2.72 – 2.69 (m, 2H, CH_2NH_2), 2.41 (s, 3H, CH_3 of bpy), 1.73 (p, J = 6.0 Hz, 2H, $CONHCH_2CH_2$), 1.62 ppm (p, J = 6.4 Hz, 2H, C$H_2CH_2NH_2$). MS (ESI^+): m/z: 447 $[M + H]^+$.

4-(*N*-(13-(3-boronobenzylamino)-4,7,10-trioxa-tridecanyl)aminocarbonyl-oxy-methyl)-4'-methyl-2,2'-bipyridine (bpy-TEG-PBA)

A mixture of bpy-TEG-NH_2 (132 mg, 0.30 mmol), 3-formylphenylboronic acid pinacol ester (79 mg, 0.34 mmol), and Et_3N (2 mL) in MeOH (15 mL) was heated to reflux under an inert atmosphere of nitrogen for 24 h. The mixture was cooled to room temperature and $NaBH_4$ (112 mg, 2.97 mmol) was added. The mixture was further stirred for 2 h and then the solvent was removed by rotary evaporation to give a colorless oil. The crude product was purified by column chromatography on silica gel using CH_2Cl_2/MeOH/NH_4OH (1:1:0.1, v/v/v) as the eluent. The product bpy-TEG-PBA was subsequently isolated as a colorless oil. Yield: 95 mg (55%). ^{1}H NMR (400 MHz, CD_3OD, 298 K, TMS): δ = 8.61 (d, J = 5.2 Hz, 1H, H6 of bpy), 8.50 (d, J = 4.8 Hz, 1H, H6' of bpy), 8.27 (s, 1H, H3 of bpy), 8.15 (s, 1H, H3' of bpy), 7.64 – 7.53 (m, 2H, H2 and H4 of phenyl ring of PBA), 7.39 (d, J = 4.8 Hz, 1H, H5 of bpy), 7.33 – 7.20 (m, 3H, H5' of bpy, H5 and H6 of phenyl ring of PBA) 5.21 (s, 2H, CH_2 on C4 of bpy), 4.10 (s, 2H, CH_2 on C1 of PBA), 3.60 – 3.50 (m, 12H, CH_2O), 3.24 (t, J = 6.8 Hz, 2H, CONHCH_2), 3.12 (t, J = 6.8 Hz, 2H, CH_2NHCH_2), 2.47 (s, 3H, CH_3 of bpy), 1.94 (t, J = 6.0 Hz, 2H, $CONHCH_2CH_2$), 1.77 ppm (t, J = 6.4 Hz, 2H, C$H_2CH_2NHCH_2$). MS (ESI^+): m/z: 581 $[M + H]^+$.

4-(*N*-(13-benzylamino-(4,7,10-trioxa-tridecanyl)aminocarbonyl)-oxy-methyl)-4'-methyl-2,2'-bipyridine (bpy-TEG-Bn)

A mixture of bpy-TEG-NH_2 (86 mg, 0.19 mmol), benzaldehyde (19.7 μL, 0.19 mmol), and Et_3N (2 mL) in MeOH (15 mL) was refluxed under an inert atmosphere of nitrogen for 24 h. The mixture was cooled to room temperature and $NaBH_4$ (73 mg, 1.93 mmol) was added. The mixture was further stirred for 2 h and then the solvent was removed by rotary evaporation to give a colorless oil. The crude product was purified by column chromatography on silica gel using CH_2Cl_2/MeOH/NH_4OH (10:1:0.1, v/v/v) as the eluent. The product bpy-TEG-Bn was subsequently isolated as a colorless oil. Yield: 87 mg (84%). ^{1}H NMR (400 MHz, CD_3OD, 298 K, TMS): δ = 8.58 (d, *J* = 5.2 Hz, 1H, H6 of bpy), 8.47 (d, *J* = 4.8 Hz, 1H, H6' of bpy), 8.26 (s, 1H, H3 of bpy), 8.12 (s, 1H, H3' of bpy), 7.35 (d, *J* = 4.4 Hz, 1H, H5 of bpy), 7.31 – 7.25 (m, 4H, H2, H3, H5 and H6 of phenyl ring), 7.24 (d, *J* = 5.2 Hz, 2H, H5' of bpy and H4 of phenyl ring of Bn), 5.19 (s, 2H, CH_2 on C4 of bpy), 3.73 (s, 2H, CH_2 on C1 of Bn), 3.56 – 3.47 (m, 12H, CH_2O), 3.23 (t, *J* = 6.8 Hz, 2H, CONHCH_2), 2.69 – 2.66 (m, 2H, CH_2NHCH_2), 2.42 (s, 3H, CH_3 of bpy), 1.80 – 1.73 ppm (m, 4H, CONHCH_2CH_2 and CH_2CH_2NHCH_2). MS (ESI$^+$): *m*/*z*: 537 [M + H]$^+$.

[Ir(ppy)$_2$(bpy-TEG-PBA)](PF$_6$) (1a)

A mixture of [Ir_2(ppy)$_4Cl_2$] (47 mg, 43.8 μmol) and bpy-TEG-PBA (50.9 mg, 87.7 μmol) in CH_2Cl_2/MeOH (25 mL, 1:4, v/v) was stirred at room temperature under an inert atmosphere of nitrogen in the dark for 24 h. The reaction mixture was cooled to room temperature and stirred for 30 min after addition of KPF_6 (8.88 mg, 48.2 μmol). The solvent was removed by rotary evaporation to give a yellow solid. Subsequent recrystallization of the solid from CH_2Cl_2/diethyl ether afforded the complex as yellow crystals. Yield: 40 mg (50%). ^{1}H NMR (400 MHz, CD_3OD, 298 K, TMS): δ = 8.71 (s, 1H, H3 of bpy), 8.66 (s, 1H, H3' of bpy), 8.14 (d, *J* = 8.4 Hz, 2H, H3 of pyridyl ring of ppy), 7.97 (d, *J* = 5.6 Hz, 1H, H6 of bpy), 7.93 – 7.83 (m, 6H, H6' of bpy, H4 and H6 of pyridyl ring of ppy, and H2 of phenyl ring of PBA), 7.65 (d, *J* = 5.6 Hz, 2H, H3 of phenyl ring of ppy), 7.52 – 7.48 (m, 2H, H5 of bpy and H4 of phenyl ring of PBA), 7.41 (d, *J* = 5.2 Hz, 1H, H5' of bpy), 7.21 – 7.02 (m, 6H, H5 of pyridyl ring and H4 of phenyl ring of ppy and H5 and H6 of phenyl ring of PBA), 6.90 (t, *J* = 7.2 Hz, 2H, H5 of phenyl ring of ppy), 6.31 (t, *J* = 6.8 Hz, 2H, H6 of phenyl ring of ppy), 5.30 (s, 2H, CH_2 on C4 of bpy), 3.97 (s, 2H, CH_2 on C1 of PBA), 3.61 – 3.51 (m, 12H, CH_2O), 3.24 (t, *J* = 6.8 Hz, 2H, CONHCH_2), 2.98 (s, 2H, CH_2NHCH_2), 2.61 (s, 3H, CH_3 of bpy), 1.94 – 1.86 (m, 2H, CONHCH_2CH_2), 1.79 – 1.76 ppm (m, 2H, CH_2CH_2NHCH_2). ^{13}C NMR (150 MHz, CD_3OD, 298 K, TMS): δ = 168.0, 162.0, 161.7, 161.5, 156.2, 155.4, 152.2, 151.0, 150.2, 152.1, 150.0, 149.6, 148.5, 142.9, 143.8, 138.2, 138.1, 131.4, 131.3, 130.1, 130.0, 128.9, 125.4, 124.6, 124.5, 123.0, 122.2, 120.0, 70.1, 70.0, 69.8, 69.7, 68.4, 63.6, 48.5, 46.2, 38.0, 29.4, 20.0 ppm. IR (KBr): $\tilde{\nu}$ = 3423 (N–H), 1719 (C=O), 843 (PF_6^-) cm^{-1}. MS (ESI$^+$): *m*/*z*: 1082 [M – PF_6^-]$^+$. Elemental analysis calcd (%) for $IrC_{52}H_{57}N_6O_7BPF_6{\cdot}H_2O{\cdot}2CH_3OH$: C 49.58, H 5.16, N 6.42; found: C 49.65, H 5.40, N 6.75.

[Ir(ppy)$_2$(bpy-TEG-Bn)](PF$_6$) (1b)

A mixture of [Ir_2(ppy)$_4Cl_2$] (43.1 mg, 40.2 μmol) and bpy-TEG-Bn (43.1 mg, 80.5 μmol) in CH_2Cl_2/MeOH (25 mL, 1:4, v/v) was stirred at room temperature under an inert atmosphere of nitrogen in the dark for 24 h. The reaction mixture was cooled to room temperature and stirred for 30 min after addition of KPF_6 (8.14 mg, 44.2 μmol). The solvent was removed by rotary evaporation to give a yellow solid. Subsequent recrystallization of the solid from CH_2Cl_2/diethyl ether afforded the complex as yellow crystals. Yield: 55 mg (58%). ^{1}H NMR (400 MHz, CD_3OD, 298 K, TMS): δ = 8.64 (s, 1H, H3 of bpy), 8.57 (s, 1H, H3' of bpy), 8.14 (d, *J* = 8.4 Hz, 2H, H3 of pyridyl ring of ppy), 7.98 (d, *J* = 5.6 Hz, 1H, H6 of bpy), 7.89 – 7.83 (m, 5H, H6' of bpy, H4 and H6 of pyridyl ring of ppy), 7.65 (d, *J* = 5.6 Hz, 2H, H3 of phenyl ring of ppy), 7.48 – 7.41 (m, 7H, H5 and H5' bpy, H2, H3, H4, H5 and H6 of phenyl ring of Bn), 7.09 – 7.03 (m, 4H, H5 of pyridyl ring and H4 of phenyl ring of ppy), 6.91 (t, *J* = 6.8 Hz, 2H, H5 of phenyl ring of ppy), 6.31 (t, *J* = 7.6 Hz, 2H, H6 of phenyl ring of ppy), 5.30 (s, 2H, CH_2 on C4 of bpy), 4.23 (s, 2H, CH_2 on C1 of Bn), 3.67 – 3.49 (m, 12H, CH_2O), 3.24 – 3.20 (m, 4H, CONHCH_2 and CH_2NHCH_2), 2.61 (s, 3H, CH_3 of bpy), 2.02 – 1.96 (m, 2H, CONHCH_2CH_2), 1.80 – 1.73 ppm (m, 2H, CH_2CH_2NHCH_2). ^{13}C NMR (150 MHz, CD_3OD, 298 K, TMS): δ = 168.0, 162.0, 161.7, 161.5, 156.2, 155.3, 152.2, 150.9, 150.3, 150.1, 149.6, 148.5, 143.9, 143.8, 138.2, 138.1, 131.5, 131.4, 130.1, 130.1, 129.4, 129.3, 129.0, 128.9, 125.3, 124.6, 124.5, 123.0, 122.2, 119.5, 70.0, 69.9, 69.8, 69.7, 68.7, 68.3, 63.6 51.0, 46.3, 37.9, 29.5, 19.9 ppm. IR (KBr): $\tilde{\nu}$ = 3428 (N–H), 1719 (C=O), 843 (PF_6^-) cm^{-1}. MS (ESI$^+$): *m*/*z*: 1038 [M – PF_6^-]$^+$. Elemental analysis calcd (%) for $IrC_{52}H_{57}N_6O_5PF_6{\cdot}4H_2O{\cdot}1.5CH_2Cl_2$: C 46.51, H 4.89, N 6.08; found: C 46.12, H 5.18, N 6.47.

[Ir(pq)$_2$(bpy-TEG-PBA)](PF$_6$) (2a)

The synthetic procedure was similar to that of complex **1a** except that [Ir_2(pq)$_4Cl_2$] (81.6 mg, 64.1 μmol) was used instead of [Ir_2(ppy)$_4Cl_2$]. The complex was isolated as orange crystals. Yield: 130 mg (76%). ^{1}H NMR (400 MHz, CD_3OD, 298 K, TMS): δ = 8.43 – 8.38 (m, 4H, H3 of quinoline of pq, H3 and H6 of bpy), 8.24 – 8.17 (m, 5H, H3' of bpy, H3 of phenyl ring and H4 of quinoline of pq), 8.10 (d, *J* = 5.6 Hz, 1H, H6' of bpy), 7.84 (d, *J* = 7.6 Hz, 2H, H8 of quinoline of pq), 7.59 – 7.22 (m, 10H, H5 and H5' of bpy, H5 and H7 of quinoline of pq, H2, H4, H5 and H6 of phenyl ring of PBA), 7.18 (t, *J* = 7.2 Hz, 2H, H4 of phenyl ring of pq), 7.08 – 7.02 (m, 2H, H6 of quinoline of pq), 6.81 (t, *J* = 7.2 Hz, 2H, H5 of phenyl ring of pq), 6.51 (t, *J* = 8.8 Hz, 2H, H6 of phenyl ring of pq), 5.14 (s, 2H, CH_2 on C4 of bpy), 4.12 (s, 2H, CH_2 on C1 of PBA), 3.61 – 3.48 (m, 12H, CH_2O), 3.21 – 3.12 (m, 4H, CONHCH_2 and CH_2NHCH_2), 2.46 (s, 3H, CH_3 of bpy), 1.97 – 1.91 (m, 2H, CONHCH_2CH_2), 1.77 – 1.71 ppm (m, 2H CH_2CH_2NHCH_2). ^{13}C NMR (150 MHz, CD_3OD, 298 K, TMS): δ = 170.3, 161.9, 156.4, 156.0, 155.2, 152.1, 150.9, 150.8, 147.6, 147.4, 147.3, 147.1, 145.8, 139.9, 139.8, 134.2, 130.5, 130.3, 128.9, 128.5, 127.8, 127.1, 127.0, 126.4, 126.3, 125.0, 124.7, 124.6, 124.5, 122.6, 121.2, 117.6, 117.5, 70.1, 69.9, 69.8, 69.7, 65.4, 63.4, 52.1, 45.9, 38.0, 29.4, 19.7 ppm. IR (KBr): $\tilde{\nu}$ = 3428 (N–H), 1718, (C=O), 845 (PF_6^-) cm^{-1}. MS (ESI$^+$): *m*/*z*: 1181 [M – PF_6^-]$^+$. Elemental analysis calcd (%) for $IrC_{60}H_{61}N_6O_7BPF_6{\cdot}2H_2O{\cdot}3CH_3OH$: C 51.89, H 5.32, N 5.76; found: C 52.17, H 5.10, N 5.99.

[Ir(pq)$_2$(bpy-TEG-Bn)](PF$_6$) (2b)

The synthetic procedure was similar to that of complex **1b** except that [Ir_2(pq)$_4Cl_2$] (50.8 mg, 39.9 μmol) was used instead of [Ir_2(ppy)$_4Cl_2$]. The complex was isolated as orange crystals. Yield: 72 mg (70%). ^{1}H NMR (400 MHz, CD_3OD, 298 K, TMS): δ = 8.43 – 8.38 (m, 4H, H3 of quinoline of pq, H3 and H6 of bpy), 8.23 – 8.16 (m, 5H, H3' of bpy, H3 of phenyl ring and H4 of quinoline of pq), 8.10 (d, *J* = 5.6 Hz, 1H, H6' of bpy), 7.84 (d, *J* =7.6 Hz, 2H, H8 of quinoline of pq), 7.50 (d, *J* = 5.6 Hz, 1H, H5 of bpy), 7.44 – 7.28 (m, 10H, H5' of bpy, H5 and H7 of quinoline of pq, H2, H3, H4, H5 and H6 of phenyl ring of Bn), 7.18 (t, *J* = 7.6 Hz, 2H, H4 of phenyl ring of pq), 7.08 – 7.02 (m, 2H, H6 of quinoline of pq), 6.81 (t, *J* = 6.8 Hz, 2H, H5 of phenyl ring of pq), 6.51 (t, *J* = 8.4 Hz, 2H, H6 of phenyl ring of pq), 5.15 (s, 2H, CH_2 on C4 of bpy), 3.87 (s, 2H, CH_2 on C1 of phenyl ring of Bn), 3.58 – 3.48 (m, 12H, CH_2O), 3.19 (t, *J* = 6.4 Hz, 2H, CONHCH_2), 2.81 (s, 2H, CH_2NHCH_2), 2.46 (s, 3H, CH_3 of bpy), 1.85 – 1.82 (m, 2H, CONHCH_2CH_2), 1.75 – 1.72 ppm (m, 2H, CH_2CH_2NHCH_2). ^{13}C NMR (150 MHz, CD_3OD, 298 K, TMS): δ = 170.4, 161.9, 161.7, 161.4, 156.0, 155.2, 152.1, 150.9, 150.8, 147.6, 147.4, 147.3, 147.1,

145.8, 139.9, 139.8, 134.2, 134.1, 130.5, 130.3, 128.9, 128.5, 128.4, 128.3, 127.8, 127.0, 126.9, 126.4, 126.3, 125.1, 124.7, 124.6, 124.5, 122.6, 121.2, 117.5, 70.1, 70.0, 69.9, 69.8, 69.3, 63.4, 52.6, 46.2, 38.0, 29.4, 19.7 ppm. IR (KBr): $\tilde{\nu}$ = 3416 (N–H), 1718, (C=O), 845 (PF_6^-) cm^{-1}. MS (ESI^+): *m/z*: 1137 [M – PF_6^-]$^+$. Elemental analysis calcd (%) for $IrC_{60}H_{60}N_6O_5PF_6{\cdot}H_2O{\cdot}CH_3OH$: C 54.99, H 4.99, N 6.31; found: C 54.73, H 5.35, N 6.73.

[Ir(pqe)$_2$(bpy-TEG-PBA)](Cl) (4a)

A mixture of $[Ir_2(pqe)_4Cl_2]$ (54 mg, 35.9 μmol) and bpy-TEG-PBA (42.0 mg, 72.4 μmol) in MeOH (15 mL) was stirred at room temperature under an inert atmosphere of nitrogen in the dark for 24 h. The solvent was removed by rotary evaporation to give a reddish brown solid. Subsequent recrystallization of the solid from CH_2Cl_2/diethyl ether afforded the complex as reddish brown crystals. Yield: 81 mg (77%). ^{1}H NMR (400 MHz, CD_3OD, 298 K, TMS): δ = 8.78 (d, *J* = 6.4 Hz, 2H, H3 of quinoline of pqe), 8.55 – 8.52 (m, 2H, H5 of quinoline of pqe), 8.26 – 8.23 (m, 3H, H3 of phenyl ring of pqe and H3 of bpy), 8.18 (d, *J* = 6.4 Hz, 1H, H6 of bpy), 8.15 (s, 1H, H3' of bpy), 8.07 (d, *J* = 6.0 Hz, 1H, H6' of bpy), 7.59 – 7.56 (m, 3H, H8 of quinoline of pqe and H5 of bpy), 7.51 – 7.43 (m, 5H, H6 of quinoline of pqe, H5' of bpy, H2 and H4 of phenyl ring of PBA), 7.36 – 7.32 (m, 2H, H5 and H6 of phenyl ring of PBA), 7.25 – 7.21 (m, 2H, H4 of phenyl ring of pqe), 7.11 – 7.07 (m, 2H, H7 of quinoline of pqe), 6.88 – 6.85 (m, 2H, H5 of phenyl ring of pqe), 6.58 – 6.53 (m, 2H, H6 of phenyl ring of pqe), 5.13 (s, 2H, CH_2 on C4 of bpy), 4.61 (s, 2H, CH_2 on C1 of PBA), 4.13 (s, 6H, $COOCH_3$), 3.62 – 3.46 (m, 12H, CH_2O), 3.19 – 3.12 (m, 4H, CONHC*H*$_2$ and C*H*$_2$NHCH$_2$), 2.46 (s, 3H, CH_3 of bpy), 1.96 – 1.93 (m, 2H, $CONHCH_2CH_2$), 1.74 – 1.71 ppm (m, 2H, $CH_2CH_2NHCH_2$). MS (ESI^+): *m/z*: 1297 [M – Cl^-]$^+$.

[Ir(pqe)$_2$(bpy-TEG-Bn)](Cl) (4b)

The synthetic procedure was similar to that of complex **4a** except that bpy-TEG-Bn (40.0 mg, 74.7 μmol) was used instead of bpy-TEG-PBA. The complex was isolated as reddish brown crystals. Yield: 90 mg (87%). ^{1}H NMR (400 MHz, CD_3OD, 298 K, TMS): δ = 8.78 (d, *J* = 5.6 Hz, 2H, H3 of quinoline of pqe), 8.53 (d, *J* = 8.0 Hz, 2H, H5 of quinoline of pqe), 8.26 – 8.15 (m, 5H, H3 of phenyl ring of pqe, H6, H3 and H3' of bpy), 8.07 (d, *J* = 5.6 Hz, 1H, H6' of bpy), 7.58 – 7.51 (m, 2H, H8 of quinoline of pqe), 7.48 – 7.41 (m, 8H, H6 of quinoline of pqe, H5 and H5' of bpy, H2, H3, H5 and H6 of phenyl ring of Bn), 7.25 – 7.17 (m, 3H, H4 of phenyl ring of pqe and H4 of phenyl ring of Bn), 7.11 – 7.05 (m, 2H, H7 of quinoline of pqe), 6.89 – 6.85 (m, 2H, H5 of phenyl ring of pqe), 6.58 – 6.53 (m, 2H, H6 of phenyl ring of pqe), 5.15 (s, 2H, CH_2 on C4 of bpy), 4.63 (s, 2H, CH_2 on C1 of Bn), 4.13 (s, 6H, $COOCH_3$), 3.63 – 3.43 (m, 12H, CH_2O), 3.19 – 3.15 (m, 4H, CONHC*H*$_2$ and C*H*$_2$NHCH$_2$), 2.46 (s, 3H, CH_3 of bpy), 1.97 – 1.94 (m, 2H, $CONHCH_2CH_2$), 1.74 – 1.71 ppm (m, 2H, $CH_2CH_2NHCH_2$). MS (ESI^+): *m/z*: 1253 [M – Cl^-]$^+$.

[Ir(pqa)$_2$(bpy-TEG-PBA)](PF$_6$)·HCl (3a)

A mixture of complex **4a** (80.0 mg, 60.0 μmol) and $LiOH{\cdot}H_2O$ (5.0 mg, 112 μmol) in THF/H_2O (12 mL) (4:1, v/v) was stirred at room temperature under an inert atmosphere of nitrogen in the dark for 2 h. The pH of the mixture was adjusted to 3 using amberlite IR120 H resin. The mixture was then filtered and the filtrate was rotary evaporated to dryness, affording a reddish brown solid. The solid was dissolved in MeOH (15 mL) containing KPF_6 (12.1 mg, 66.0 μmol) and the solution was stirred at room temperature under an inert atmosphere of nitrogen in the dark for 30 min. The solvent was then removed by rotary evaporation to give a reddish brown solid. Subsequent recrystallization of the solid from MeOH/diethyl ether afforded the complex as red crystals. Yield: 67 mg (84%). ^{1}H NMR (400 MHz, CD_3OD, 298 K, TMS): δ = 8.68 (d, *J* = 7.2 Hz, 2H, H3 of quinoline of pqa), 8.51 (t, *J* = 8.0 Hz, 2H, H5 of quinoline of pqa), 8.23 – 8.21 (m, 4H, H3 of phenyl ring of pqa and H6 and H3 of bpy), 8.15 (s, 1H, H3' of bpy), 8.10 (d, *J* = 5.6 Hz, 1H, H6' of bpy), 7.76 – 7.41 (m, 10H, H5 and H5' of bpy, H6 and H8 of quinoline of pqa, H2, H4, H5 and H6 of phenyl ring of PBA), 7.21 (t, *J* = 7.2 Hz, 2H, H4 of phenyl ring of pqa), 7.09 – 7.02 (m, 2H, H7 of quinoline of pqa), 6.85 (t, *J* = 7.2 Hz, 2H, H5 of phenyl ring of pqa), 6.56 (t, *J* = 8.4 Hz, 2H, H6 of phenyl ring of pqa), 5.20 – 5.11 (m, 2H, CH_2 on C4 of bpy), 4.23 (s, 2H, CH_2 on C1 of of PBA), 3.64 – 3.46 (m, 12H, CH_2O), 3.22 – 3.16 (m, 4H, CONHC*H*$_2$ and C*H*$_2$NHCH$_2$), 2.46 (s, 3H, CH_3 of bpy), 2.00 – 1.97 (m, 2H, $CONHCH_2CH_2$), 1.74 – 1.71 (m, 2H, $CH_2CH_2NHCH_2$). ^{13}C NMR (150 MHz, CD_3OD, 298 K, TMS): δ = 170.1, 167.8, 161.9, 16.6, 161.4, 156.4, 155.9, 150.0, 152.4, 150.8, 150.7, 148.0, 147.9, 147.5, 147.0, 145.6, 145.5, 134.4, 134.3, 130.7, 130.4, 129.4, 128.8, 128.2, 127.2, 127.1, 127.0, 126.9, 125.3, 125.1, 125.0, 124.5, 124.4, 124.4, 122.9, 121.3, 117.4, 117.2, 70.0, 69.8, 69.8, 68.7, 68.7, 68.3, 63.3, 51.0, 46.2, 37.9, 29.5, 19.8 ppm. IR (KBr): $\tilde{\nu}$ = 3416 (N–H), 3046 (O–H), 1723 (C=O), 847 (PF_6^-) cm^{-1}. MS (ESI^-): *m/z*: 1267 [M – 2 × H – PF_6^- – HCl]$^-$. Elemental analysis calcd (%) for $IrC_{62}H_{62}N_6O_{11}BClPF_6{\cdot}H_2O{\cdot}3MeOH$: C 49.89, H 4.90, N 5.37; found: C 50.11, H 5.26, N 5.55.

[Ir(pqa)$_2$(bpy-TEG-Bn)](PF$_6$)·HCl (3b)

The synthetic procedure was similar to that of complex **3a** except that complex **4b** was used instead of complex **4a**. The complex was isolated as red crystals. Yield: 64 mg (77%). ^{1}H NMR (400 MHz, CD_3OD, 298 K, TMS): δ = 8.68 (d, *J* = 5.2 Hz, 2H, H3 of quinoline of pqa), 8.51 (t, *J* = 8.0 Hz, 2H, H5 of quinoline of pqa), 8.23 – 8.21 (m, 4H, H3 of phenyl ring of pqa and H6 and H3 of bpy), 8.15 (s, 1H, H3' of bpy), 8.10 (d, *J* = 6.0 Hz, 1H, H6' of bpy), 7.56 – 7.41 (m, 11H, H6 and H8 of quinoline of pqa, H5 and H5' of bpy, and H2, H3, H4, H5 and H6 of phenyl ring of Bn), 7.22 (t, *J* = 7.2 Hz, 2H, H4 of phenyl ring of pqa), 7.09 – 7.02 (m, 2H, H7 of quinoline of pqa), 6.85 (t, *J* = 7.2 Hz, 2H, H5 of phenyl ring of pqa), 6.56 (t, *J* = 8.0 Hz, 2H, H6 of phenyl ring of pqa), 5.20 – 5.11 (m, 2H, CH_2 on C4 of bpy), 4.23 (s, 2H, CH_2 on C1 of Bn), 3.64 – 3.47 (m, 12H, CH_2O), 3.22 – 3.17 (m, 4H, CONHC*H*$_2$ and C*H*$_2$NHCH$_2$), 2.47 (s, 3H, CH_3 of bpy) 2.00 – 1.97 (m, 2H, $CONHCH_2CH_2$), 1.76 – 1.71 (m, 2H, $CH_2CH_2NHCH_2$) ^{13}C NMR (150 MHz, CD_3OD, 298 K, TMS): δ = 170.1, 167.8, 161.9, 161.7, 161.4, 156.4, 155.9, 155.0, 152.4, 151.1, 150.8, 150.7, 148.1, 147.9, 147.6, 147.0, 145.6, 145.5, 142.3, 134.4, 134.3, 131.2, 130.7, 130.4, 129.4, 129.3, 129.0, 128.8, 127.2, 127.1, 127.0, 126.9, 126.9, 125.3, 125.1, 125.0, 124.5, 124.4, 124.4, 122.9, 121.3, 117.4, 117.2, 70.1, 69.9, 69.8, 69.7, 68.6, 68.3, 63.4, 50.9, 46.1, 37.9, 29.4, 25.5, 19.8 ppm. IR (KBr): $\tilde{\nu}$ = 3422 (N–H), 3049 (O–H), 1719 (C=O), 844 (PF_6^-) cm^{-1}. MS (ESI^-): *m/z*: 1223 [M – 2 × H – PF_6^-– HCl]$^-$. Elemental analysis calcd (%) for $IrC_{62}H_{61}N_6O_9ClPF_6{\cdot}H_2O{\cdot}3MeOH$: C 51.33, H 4.97, N 5.53; found: C 50.99, H 5.29, N 5.80.

Sugar-binding studies

In the spectrophotometric titrations, the iridium(III) complex (50 μM) in 50 mM potassium phosphate buffer at pH 7.4/DMSO (9:1, v/v) was titrated with sugar of interest, which was dissolved in the same solvent mixture. The electronic absorption spectrum of the solution was measured after successive additions (2-μL aliquots) of the sugar solution at 1-min intervals. The binding constants, K_b, of the sugar to the iridium(III) complex as described in the following equilibrium assuming 1:1 complexation:

$$\mathrm{Ir} + \mathrm{Sugar} \rightleftharpoons \mathrm{Ir-Sugar}$$

was determined by fitting the titration data to the following equation:[18]

$$\frac{A_o}{(A_o - A)} = \left(\frac{\varepsilon_o}{\varepsilon_o - \varepsilon}\right)\left[\left(\frac{1}{K_b[\text{Sugar}]}\right) + 1\right]$$

where A_o and A are the dilution effect-corrected absorbance of Ir in the absence and presence of sugar at a concentration [Sugar], and ε_o and ε are the absorption coefficients for the free and sugar-bound iridium(III) complex, respectively. The K_b was determined from the ratio of the *y*-intercept to the slope of the linear fit plot of $A_o/(A_o - A)$ vs. $[\text{Sugar}]^{-1}$.

pH-dependent emission studies

A 20 mL stock solution of the iridium(III) complex (50 μM) in a mixture of 10 mM KOH and 100 mM KCl(aq)/MeOH (7:3 or 9:1, v/v) was prepared. The pH of the stock solution was adjusted to a desired value by addition of appropriate amounts of 10, 5, 2.5, 1.25, 0.5, 0.25, 0.13, 0.07, 0.04 or 0.02 N HCl(aq). After that, 2 mL of the stock solution was transferred to a quartz cuvette and the emission spectrum was measured. The solution was then returned to the stock, and the pH was further adjusted. The apparent pK_a values of the complexes were determined from the nonlinear least-square fits of the titration curves (errors based on statistical fitting).

Lipophilicity

The lipophilicity (log $P_{o/w}$) of the iridium(III) complexes was determined using the shake-flask method.[35] An aliquot of a stock solution of the complex in octan-1-ol (saturated with 0.9% NaCl, w/v) was added to an equal volume of aqueous NaCl (0.9%, w/v) (saturated with octan-1-ol). The mixture was swirled at 60 rpm for 30 min, and subsequently allowed to partitioning at 298 K. The solution was then centrifuged, and the amounts of complex in the organic layer ($[\text{Ir}]_o$) was determined by fluorescence spectroscopy. The partition coefficient ($P_{o/w}$) for each complex was calculated as the ratio of $[\text{Ir}]_o/[\text{Ir}]_w$, where $[\text{Ir}]_w$ was obtained by subtraction of the total amount of complex by the amount in the organic phase after partitioning.

Cell cultures

HepG2 and HEK293T cells were cultured in high glucose DMEM supplemented with 10% FBS and 1% penicillin-streptomycin in a humidified chamber at 37°C under a 5% CO_2 atmosphere. They were subcultured every 2 to 3 days.

Photocytotoxicity assays

HepG2 cells were seed in two 96-well flat-bottomed microplates (≈ 10,000 cells $well^{-1}$) in growth medium (100 μL) and incubated at 37°C under a 5% CO_2 atmosphere for 24 h. The iridium(III) complexes (25 μM) were then added to the wells in growth medium/DMSO (99:1, v/v). After incubation for 1 h, the culture medium was removed, the cells were washed with PBS, and phenol red-free growth medium (100 μL) was added to each well. One of the microplates was irradiated at λ = 365 nm with a 6 W UV-A lamp (Spectroline, USA) for 10 min while the other one was kept in the dark for 10 min. The cells were then replenished with fresh growth medium and further incubated for 24 h. The cell viability was assessed using the MTT assay.[27]

Acknowledgements

We thank the Hong Kong Research Grants Council (Project Nos. T42-103/16-N and CityU 11302116) and the Hong Kong Research Grants Council, National Natural Science Foundation of China (Project No. N_CityU113/15) for financial support. W.H.-T.L and L.C.-C.L. both acknowledge the receipt of a Postgraduate Studentship, a Research Tuition Scholarship, and an Outstanding Academic Performance Award administrated by City University of Hong Kong. K. K.-W. Lo is grateful to the Croucher Foundation for the award of a Croucher Senior Research Fellowship.

Keywords: imaging agents • iridium • luminescent probes • phenylboronic acid • sialic acids

[1] I. Martinez-Duncker, R. Salinas-Marin, C. Martinez-Duncker, *Int. J. Mol. Imaging* **2011**, *2011*, 1–10.

[2] a) P. R. Crocker, *Curr. Opin. Struct. Biol.* **2002**, *12*, 609–615; b) A. Varki, T. Angata, *Glycobiology* **2006**, *16*, 1R–27R; c) P. R. Crocker, J. C. Paulson, A. Varki, *Nat. Rev. Immunol.* **2007**, *7*, 255–266; d) R. Schauer, *Curr. Opin. Struct. Biol.* **2009**, *19*, 507–514; e) B. Wang, *Annu Rev. Nutr.* **2009**, *29*, 177–222.

[3] a) H. Läubli, J. L. Stevenson, A. Varki, N. M. Varki, L. Borsig, *Cancer Res.* **2006**, *66*, 1536–1542; b) N. M. Varki, A. Varki, *Lab. Invest.* **2007**, *87*, 851–857.

[4] H. Koprowski, M. Herlyn, Z. Steplewski, H. F. Sears, *Science* **1981**, *212*, 53–55.

[5] a) N. Shibuya, I. J. Goldstein, W. F. Broekaert, M. Nsimba-Lubaki, B. Peeters, W. J. Peumans, *J. Biol. Chem.* **1987**, *262*, 1596–1601; b) W. C. Wang, R. D. Cummings, *J. Biol. Chem.* **1988**, *263*, 4576–4585; c) E. C. M. Brinkman-Van der Linden, J. L. Sonnenburg, A. Varki, *Anal. Biochem.* **2002**, *303*, 98–104; d) N. Sharon, H. Lis, *Glycobiology* **2004**, *14*, 53R–62R; e) N. Sharon, *J. Biol. Chem.* **2007**, *282*, 2753–2764.

[6] a) Y. Zeng, T. N. C. Ramya, A. Dirksen, P. E. Dawson, J. C. Paulson, *Nat. Methods* **2009**, *6*, 207–209; b) J. A. Key, C. Li, C. W. Cairo, *Bioconjugate Chem.* **2012**, *23*, 363–371.

[7] a) Q. Peng, F. Chen, Z. Zhong, R. Zhuo, *Chem. Commun.* **2010**, *46*, 5888–5890; b) F. Chen, Z. Zhang, M. Cai, X. Zhang, Z. Zhong, R. Zhuo *Macromol. Biosci.* **2012**, *12*, 962–969.

[8] a) A. Liu, S. Peng, J. C. Soo, M. Kuang, P. Chen, H. Duan, *Anal. Chem.* **2011**, *83*, 1124–1130; b) W. Zhang, X.-W. He, Y.-Q. Yang, W.-Y. Li, Y.-K. Zhang, *J. Mater. Chem. B* **2013**, *1*, 347–352; c) C.-S. Chen, X.-D. Xu Y. Wang, J. Yang, H.-Z. Jia, H. Cheng, C.-C. Chu, R.-X. Zhuo, X.-Z. Zhang, *Small* **2013**, *9*, 920–926; d) L. Cheng, X. Zhang, Z. Zhang, H. Chen, S. Zhang, J. Kong, *Talanta* **2013**, *115*, 823–829; e) L.-L. Huang, Y.-J. Jin, D. Zhao, C. Yu, J. Hao, H.-Y. Xie, *Anal. Bioanal. Chem.* **2014**, *406*, 2687–2693.

[9] a) H. Otsuka, E. Uchimura, H. Koshino, T. Okano, K. Kataoka, *J. Am. Chem. Soc.* **2003**, *125*, 3493–3502; b) W. Yang, H. Fan, X. Gao, S. Gao, V. V. R. Karnati, W. Ni, W. B. Hooks, J. Carson, B. Weston, B. Wang, *Chem. Biol.* **2004**, *11*, 439–448; c) M. Regueiro-Figueroa, K. Djanashvili, D. Esteban-Gómez, A. de Blas, C. Platas-Iglesias, T. Rodríguez-Blas, *Eur. J. Org. Chem.* **2010**, 3237–3248; d) S. Deshayes, H. Cabral, T. Ishii, Y. Miura, S. Kobayashi, T. Yamashita, A. Matsumoto Y. Miyahara, N. Nishiyama, K. Kataoka, *J. Am. Chem. Soc.* **2013**, *135*, 15501–15507; e) X.-D. Xu, H. Cheng, W.-H. Chen, S.-X. Cheng, R.-X. Zhuo, X.-Z. Zhang, *Sci. Rep.* **2013**, *3*, 2679.

[10] a) L. Frullano, J. Rohovec, S. Aime, T. Maschmeyer, M. I. Prata, J. J. Pedroso de Lima, C. F. G. C. Geraldes, J. A. Peters, *Chem. Eur. J.* **2004**, *10*, 5205–5217; b) K. Djanashvili, G. A. Koning, A. J. G. M. van der Meer, H. T. Wolterbeek, J. A. Peters, *Contrast Media Mol. Imaging* **2007**, *2*, 35–41; c) M. Regueiro-Figueroa, K. Djanashvili, D. Esteban-

Gómez, T. Chauvin, É. Tóth, A. de Blas, T. Rodríguez-Blas, C. Platas-Iglesias, *Inorg. Chem.* **2010**, *49*, 4212–4223; d) C. F. G. C. Geraldes, K. Djanashvili, J. A. Peters, *Future Med. Chem.* **2010**, *2*, 409–425; e) S. Geninatti Crich, D. Alberti, I. Szabo, S. Aime, K. Djanashvili, *Angew. Chem. Int. Ed.* **2013**, *52*, 1161–1164; *Angew. Chem.* **2013**, *125*, 1199–1202; f) E. R. Neil, D. Parker, *RSC Adv.* **2017**, *7*, 4531–4540.

[11] K. K.-W. Lo, *Acc. Chem. Res.* **2015**, *48*, 2985–2995.

[12] a) K. K.-W. Lo, J. S.-W. Chan, L.-H. Lui, C.-K. Chung, *Organometallics* **2004**, *23*, 3108–3116; b) K. Y. Zhang, K. K.-W. Lo, *Inorg. Chem.* **2009**, *48*, 6011–6025; c) R. A. Smith, E. C. Stokes, E. E. Langdon-Jones, J. A. Platts, B. M. Kariuki, A. J. Hallett, S. J. A. Pope, *Dalton Trans.* **2013**, *42*, 10347–10357.

[13] K. K.-W. Lo, J. S.-Y. Lau, *Inorg. Chem.* **2007**, *46*, 700–709.

[14] a) I. M. Dixon, J.-P. Collin, J.-P. Sauvage, L. Flamigni, S. Encinas, F. Barigelletti, *Chem. Soc. Rev.* **2000**, *29*, 385–391; b) E. Baranoff, J.-P. Collin, L. Flamigni, J.-P. Sauvage, *Chem. Soc. Rev.* **2004**, *33*, 147–155; c) L. Flamigni, A. Barbieri, C. Sabatini, B. Ventura, F. Barigelletti, *Top. Curr. Chem.* **2007**, *281*, 143–203; d) Y. You, S. Y. Park, *Dalton Trans.* **2009**, 1267–1282; e) Y. Chi, P.-T. Chou, *Chem. Soc. Rev.* **2010**, *39*, 638–655; f) K. K.-W. Lo, S. P.-Y. Li, K. Y. Zhang, *New J. Chem.* **2011**, *35*, 265–287.

[15] a) S. Sprouse, K. A. King, P. J. Spellane, R. J. Watts, *J. Am. Chem. Soc.* **1984**, *106*, 6647–6653; b) A. P. Wilde, R. J. Watts, *J. Phys. Chem.* **1991**, *95*, 622–629; c) M. Maestri, V. Balzani, C. Deuschel-Cornioley, A. Von Zelewsky, *Adv. Photochem.* **1992**, *17*, 1–68.

[16] K. K.-W. Lo, C.-K. Chung, T. K.-M. Lee, L.-H. Lui, K. H.-K. Tsang, N. Zhu, *Inorg. Chem.* **2003**, *42*, 6886–6897.

[17] R. K. Murray, D. K. Granner, P. A. Mayes, V. W. Rodwell in *Harper's Illustrated Biochemistry*, 26th ed, The McGraw-Hill Companies, Inc., U.S.A., **2003**.

[18] V. W.-W. Yam, A. S.-F. Kai, *Chem. Commun.* **1998**, 109–110.

[19] G. Springsteen, B. Wang, *Tetrahedron* **2002**, *58*, 5291–5300.

[20] a) T. A. Houston, *ChemBioChem* **2010**, *11*, 954–957; b) J. A. Peters, *Coord. Chem. Rev.* **2014**, *268*, 1–22.

[21] a) J. O. Edwards, R. J. Sederstrom, *J. Phys. Chem.* **1961**, *65*, 862–863; b) R. M. Smith, A. E. Martell in *Critical Stability Constants, Vol. 2: Amines*, Plenum Press, New York, **1975**.

[22] J. Weng, Q. Mei, W. Jiang, Q. Fan, B. Tong, Q. Ling, W. Huang, *Analyst* **2013**, *138*, 1689–1699.

[23] a) M. Licini, J. A. G. Williams, *Chem. Commun.* **1999**, 1943–1944; b) T. S.-M. Tang, K.-K. Leung, M.-W. Louie, H.-W. Liu, S. H. Cheng, K. K.-W. Lo, *Dalton Trans.* **2015**, 44, 4945–4956.

[24] K. Y. Zhang, K. K.-S. Tso, M.-W. Louie, H.-W. Liu, K. K.-W. Lo, *Organometallics* **2013**, *32*, 5098–5102.

[25] a) X. Ning, J. Guo, M. A. Wolfert, G.-J. Boons, *Angew. Chem. Int. Ed.* **2008**, *47*, 2253–2255; *Angew. Chem.* **2008**, *120*, 2285–2287; b) J. C. Jewett, E. M. Sletten, C. R. Bertozzi, *J. Am. Chem. Soc.* **2010**, *132*, 3688–3690; c) K. K.-W. Lo, B. T.-N. Chan, H.-W. Liu, K. Y. Zhang, S. P.-Y. Li, T. S.-M. Tang, *Chem. Commun.* **2013**, *49*, 4271–4273; d) A. W.-T. Choi, H.-W. Liu, K. K.-W. Lo, *J. Inorg. Biochem.* **2015**, *148*, 2–10; e) T. S.-M. Tang, A. M.-H. Yip, K. Y. Zhang, H.-W. Liu, P. L. Wu, K. F. Li, K. W. Cheah, K. K.-W. Lo, *Chem. Eur. J.* **2016**, *22*, 9649–9659.

[26] M. A. Hollingsworth, B. J. Swanson, *Nat. Rev. Cancer* **2004**, *4*, 45–60.

[27] T. Mosmann, *J. Immunol. Methods* **1983**, *65*, 55–63.

[28] a) E. Reaven, L. Tsai, S. Azhar, *J. Biol. Chem.* **1996**, *271*, 16208–16217; b) C. A. Puckett, R. J. Ernst, J. K. Barton, *Dalton Trans.* **2010**, *39*, 1159–1170.

[29] a) T. Kobayashi, Y. Arakawa, *J. Cell Biol.* **1991**, *113*, 235–244; b) R. E. Pagano, O. C. Martin, H. C. Kang, R. P. Haugland, *J. Cell Biol.* **1991**, *113*, 1267–1279.

[30] D. H. Dube, C. R. Bertozzi, *Nat. Rev. Drug Discov.* **2005**, *4*, 477–488.

[31] W. L. F. Armarego, C. L. L. Chai in *Purification of Laboratory Chemicals*, 6th ed, Elsevier, Oxford, **2009**.

[32] a) B. M. Peek, G. T. Ross, S. W. Edwards, G. J. Meyer, T. J. Meyer, B. W. Erickson, *Int. J. Pept. Protein Res.* **1991**, *38*, 114–123; b) H. Zhou, P. Jiao, L. Yang, X. Li, B. Yan, *J. Am. Chem. Soc.* **2011**, *133*, 680–682; c) L. Margarucci, A. Tosco, R. De Simone, R. Riccio, M. C. Monti, A. Casapullo, *ChemBioChem* **2012**, *13*, 982–986.

[33] a) G. A. Crosby, J. N. Demas, *J. Phys. Chem.* **1971**, *75*, 991–1024; b) T. Tsutsui, M.-J. Yang, M. Yahiro, K. Nakamura, T. Watanabe, T. Tsuji, Y. Fukuda, T. Wakimoto, S. Miyaguchi, *Jpn. J. Appl. Phys.* **1999**, *38*, L1502–L1504.

[34] a) J. S.-Y. Lau, P.-K. Lee, K. H.-K. Tsang, C. H.-C. Ng, Y.-W. Lam, S.-H. Cheng, K. K.-W. Lo, *Inorg. Chem.* **2009**, *48*, 708–718; b) P.-K. Lee, H.-W. Liu, S.-M. Yiu, M.-W. Louie, K. K.-W. Lo, *Dalton Trans.* **2011**, *40*, 2180–2189.

[35] M. J. McKeage, S. J. Berners-Price, P. Galettis, R. J. Bowen, W. Brouwer, L. Ding, L. Zhuang, B. C. Baguley, *Cancer Chemother. Pharmacol.* **2000**, *46*, 343–350.

10.1002/asia.201700359

WILEY-VCH

Entry for the Table of Contents

FULL PAPER

We report here three luminescent cyclometalated iridium(III) bipyridine–PBA complexes that are capable of binding sialic acid residues, which are overexpressed on tumors. With suitable modification of their molecular structures, these complexes have a high potential to be developed as novel theranostic reagents.

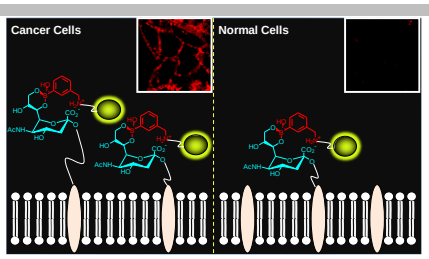

*Hua-Wei Liu, Wendell Ho-Tin Law, Lawrence Cho-Cheung Lee, Jonathan Chun-Wai Lau, and Kenneth Kam-Wing Lo**

Page No. – Page No.

Cyclometalated Iridium(III) Bipyridine–Phenylboronic Acid Complexes as Luminescent Probes for Sialic Acids and Bioimaging Reagents